materials

MDPI

Article

The Influence of Li^+ and K^+ Added Cations and Annealing Temperature on the Magnetic and Dielectric Properties of Mg-Zn Ferrite

Iulian Petrila [1] and Florin Tudorache [2,*]

[1] Faculty of Automatic Control and Computer Engineering, Gheorghe Asachi Technical University of Iasi, Boulevard Dimitrie Mangeron, No. 67, 700050 Iasi, Romania; iulianpetrila@yahoo.com
[2] Institute of Interdisciplinary Research, Department of Exact and Natural Sciences, Ramtech Center, Alexandru Ioan Cuza University of Iasi, Boulevard Carol I, No. 11, 700506 Iasi, Romania
* Correspondence: florin.tudorache@uaic.ro

Abstract: This paper presents the results of an investigation on the magnetic and dielectric properties of $Mg_{0.5}Zn_{0.5}Fe_2O_4$ spinel ferrite with a 1% weight percentage of Li^+ and K^+ added cations. The addition of metal ions plays an important role in increasing the porosity and favors the formation of ferrite at low temperatures. The goal of this new research is to demonstrate that by selecting the type of metallic cations for addition or choosing an optimal sintering temperature, it may be possible to improve the magnetic and electrical properties of Mg-Zn ferrite. The samples were prepared using sol-gel self-combustion techniques and annealed at 1000 °C, 1100 °C, and 1200 °C. Scanning electron microscopy revealed the shape and grain size of the samples, and the phase composition was analyzed using the X-ray diffraction technique. The magnetic information, such as remanent magnetization M_R, saturation magnetization M_S, and coercivity H_C, were extracted from the hysteresis loops of the samples. The electrical investigation was focused on the low- and high-frequency dependence of dielectric constant and dielectric losses. The results are discussed in terms of microstructural changes induced by the additions of Li^+ and K^+ metallic cations. Conclusions are drawn concerning the optimization of magnetic and electrical properties for the development of Mg-Zn ferrite with possible applications in the field of magnetic materials or electronics.

Keywords: magnesium-zinc ferrite; hysteresis loops; dielectric permittivity; coercivity

check for updates

Citation: Petrila, I.; Tudorache, F. The Influence of Li^+ and K^+ Added Cations and Annealing Temperature on the Magnetic and Dielectric Properties of Mg-Zn Ferrite. *Materials* **2021**, *14*, 4916. https://doi.org/10.3390/ma14174916

Academic Editor: Tao-Hsing Chen

Received: 20 July 2021
Accepted: 26 August 2021
Published: 29 August 2021

Publisher's Note: MDPI stays neutral with regard to jurisdictional claims in published maps and institutional affiliations.

Copyright: © 2021 by the authors. Licensee MDPI, Basel, Switzerland. This article is an open access article distributed under the terms and conditions of the Creative Commons Attribution (CC BY) license (https://creativecommons.org/licenses/by/4.0/).

1. Introduction

Ferrites based on Mg-Zn are important ceramic materials that present spinel-type lattices with soft magnetic properties.There isenhanced interest in these materials due to their chemical stability and low production costs for possible applications such as magnetic recording, electromagnets, hyperthermia treatment, antibacterial activity, humidity sensors, medicine, and inductive sensors and actuators working in a wide frequency range 10^2 to 10^9 Hz [1–6].

The main inconvenience of spinel magnesium-based ceramic materials is their high annealing temperature, over 1300 °C, which causes significant material loss and large energy consumption. Magnetic and dielectric properties of ferrites can be enhanced or altered by modifying various added metallic cations and the sintering temperature and/or time [7–11]. Magnetic and dielectric properties of spinel ferrites AB_2O_4 are also dependent on the distribution of A and B cations in tetrahedral or octahedral sites, respectively. The various cationic distributions were studied by different authors and reported in various papers [12–16]. The common conclusion of these works was that the temperature of synthesis influences the distribution of metal cations in the position of the spinel network. The Mg^{2+} cations are usually placed on octahedral sites, and only a minority are placed in tetrahedral sites of sublattice [17,18].

The main goal of this work is to investigate the evolution of the magnetic and dielectric properties of magnesium-zinc ferrite as a result of the addition of two alkaline metallic cations with the same valences Li^+ and K^+. The addition of alkaline metal cations of Li^+ and K^+ to the base structure of the magnesium-zinc ferrite was chosen because alkaline metals present a high reactivity and special physico-chemical properties, which can easily integrate into the structure of ferrite. Because alkaline metals are very reactive, they have a single electron on the last layer, which they readily give up to other metals in the ferrite composition. The addition of metal cations to the magnesium-zinc ferrite structure can make an essential contribution to improvingthe conduction mechanism, optical or magnetic properties of semiconductors [19–21].

Magnetic and dielectric properties at room temperatures for Mg-Zn ferrites were reported by various authors [22–25]. High dielectric permittivity values can be reached using oxides of transition elements, and this is the main reason for the synthesis of Mg-Zn ferrites with Li^+ and K^+ added cations. Controlling the microstructure and selecting the intrinsic resistivity are the most important factors for achieving good values of permittivity, above $\varepsilon_r > 1000$.

Therefore, the preparation technique and the sintering conditions of the samples were considered to be very important. We selected Mg-Zn ferrite for the following reasons: it is a lighter ceramic material, and the stability of the Mg^{2+} ion avoids the appearance of Fe^{2+} ions (an essential requirement to obtain good values of permittivity); magnesium-zinc ferrite has the largest application field including, magnetic materials, electronics, or sensors; it is relatively easy to prepare, and all the materials involved in the preparation of ferrite are friendly for the environment.

2. Materials and Methods

Various preparation methods were used to obtain Mg-Zn ferrite, such as sol–gel, sol-gel auto-combustion, co-precipitation, and thermal evaporation [26–30]. Reference samples with stoichiometric composition $Mg_{0.5}Zn_{0.5}Fe_2O_4$ were prepared in an air atmosphere by using the sol-gel self-combustion method [31]. For the preparation of ferrite by the sol-gel self-combustion method, we have chosen the nitrate because ammonia and polyvinyl alcohol can form, in some ratios and in the dry state, pyrotechnic mixtures in which ammonia is the oxidant, and polyvinyl alcohol is combustible. Such a mixture, once ignited, undergoes an exothermic and self-sustaining reaction that generates a sufficient amount of heat to eliminate the water. Calculations were carried out to obtain 0.05 moles of ferrite $Mg_{0.5}Zn_{0.5}Fe_2O_4$ resulting in the following amounts of nitrates: $Mg(NO_3)_2{\cdot}6H_2O$ = 6.075 cm^3; $Zn(NO_3)_2{\cdot}6H_2O$ = 16.34 cm^3; $Fe(NO_3)_3{\cdot}9H_2O$ = 55.8 cm^3, and polyvinyl alcohol = 80.61 cm^3. Required quantities of high-grade purity precursors $Mg(NO_3)_2{\cdot}6H_2O$; $Zn(NO_3)_2{\cdot}6H_2O$; $Fe(NO_3)_3{\cdot}9H_2O$ and polyvinyl alcohol $[CH_2CHOH]_n$ from Sigma–Aldrich, was weighed according to the stoichiometric formula of desired final composition and dissolved in small amounts of distilled water. Polyvinyl alcohol solution was added in molar ratio 1:1 to make a colloidal solution. The constituents were mixed and neutralized (pH = 7) with solution 10% ammonia (NH_4OH) concentration. To initiate an ignition combustion reaction, each resulting mixture composition was dried for 4 h at 100 °C and, after combustion, resulted in $Mg_{0.5}Zn_{0.5}Fe_2O_4$ ferrite powder.

Equal amounts of Li_2CO_3 = 1.0221g and K_2CO_3 = 1.0221g powders as a source of Li^+ and K^+ cations were added and mixed with the magnesium-zinc ferrite composition.

Since the self-combustion reaction cannot be complete in the whole mass of material, a primary pre-calcining treatment wasrequired, which was carried out for 1 h at 500 °C in an air atmosphere. Desired shapes of specimens (6 mm diameter and 1–2 mm thickness pellets) were obtained by uniaxially pressing the pre-calcined powder at 5×10^7 N/m^2 using a Carver model 4350 hydraulic press. In order to obtain the best homogeneity of the mixture between the ferrite and the addition of metal cations, the heat treatment was carried out for 4 h.

In order to observe the influence of annealing temperature on structural, magnetic, and dielectric properties of compacts specimens, three different temperatures were chosen for the thermal treatment: 1000 °C, 1100 °C, and 1200 °C, respectively, for 4 h. The internal mechanical stresses that can occur by thermal shocks were avoided using a slow sample cooling process at the end of each treatment. A mechanical polishing ensured the planarity and the parallelism of the faces of the sample and deposition of thin silver contact electrodes on both faces.

The phase components analysis was performed at room temperature using a Shimadzu LabX-6000 X-ray diffractometer with Bragg-Brentano focusing system and CuKα radiation (α = 1.5405 Å) source.

The SEM images were obtained using a scanning electron microscope model Quanta 200 on freshly fractured samples. The investigation was focused on crystallite agglomeration tendencies and crystallites' mean size. The roughness of the surface was performed using the 3D optical surface profilometer model ZygoZeGage.

The investigations of magnetic properties were performed on a vibrating sample magnetometer (VSM) at room temperature. For these measurements, the 4 mm diameter spherical samples were fabricated by mechanical polishing. The maximum intensity of the magnetic field was 900 kA/m.

The dependence of electrical permittivity on the frequency was recorded using a Wayne Kerr Impedance Phase Analyzer 6400P in the range of 1 Hz–1 MHz.

3. Results and Discussion

The effect of the addition of Li^+ and K^+ cations in the Mg-Zn ferrite is discussed in terms of sintering behavior, structure evolution, magnetical properties improvement, and dielectric characterization of these materials.

3.1. Microstructural Characterization

Comparative analysis of recorded X-ray diffractograms (Figure 1) emphasized the spinel structure—cubic phase of each sample: reference, Li^+ and K^+ samples. Diffraction lines belonging to the spinel phase are identified, the highest intensity peak (311) is present at 2θ = 36°, and all diffractograms have confirmed the single-phase character of samples, similar to ones reported in the literature [32–35].

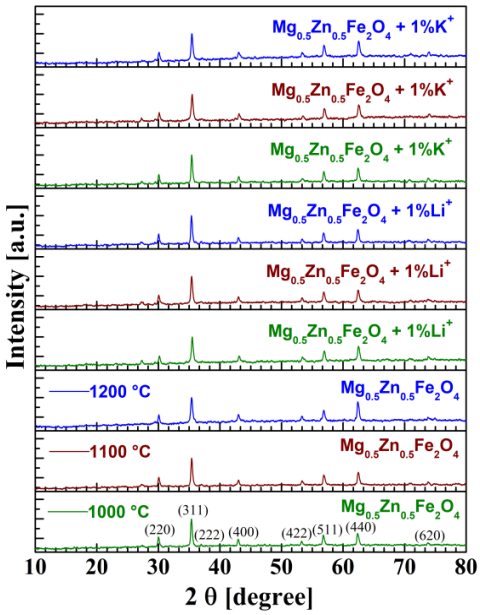

Figure 1. XRD patterns of magnesium-zinc ferrites.

We also observed that increasing the annealing temperature allowed the decrease of the porosity of the samples. From the geometrical dimensions and the weight of each sample, we present in Table 1 the calculated porosity values of Mg-Zn ferrites. A slight increase in the porosity of the samples with cations additions in comparison with the basic ferrite was observed. In the case of Mg-Zn ferrite sintered at 1000 °C, the addition of Li^+ cations caused an increase in porosity of 3%, and the addition of K^+ cations caused an increase in porosity of 9%. A significant increase in porosity wasobserved for ferrites sintered at 1200 °C, where the addition of Li^+ cations caused an increase in porosity of 20% and the addition of K^+ cations caused an increase in porosity of 35%. The increase can be explained bases on the atomic radius of the substituent cations. Similar results about the evolution of porosity were reported in the literature by [32].

Table 1. The porosity of Mg-Zn ferrites.

Sample	Annealing Temperature [°C]	Porosity [%]
$Mg_{0.5}Zn_{0.5}Fe_2O_4$	1000	32
$Mg_{0.5}Zn_{0.5}Fe_2O_4$	1100	29
$Mg_{0.5}Zn_{0.5}Fe_2O_4$	1200	20
$Mg_{0.5}Zn_{0.5}Fe_2O_4$ + 1%Li^+	1000	33
$Mg_{0.5}Zn_{0.5}Fe_2O_4$ + 1%Li^+	1100	31
$Mg_{0.5}Zn_{0.5}Fe_2O_4$ + 1%Li^+	1200	24
$Mg_{0.5}Zn_{0.5}Fe_2O_4$ + 1%K^+	1000	35
$Mg_{0.5}Zn_{0.5}Fe_2O_4$ + 1%K^+	1100	31
$Mg_{0.5}Zn_{0.5}Fe_2O_4$ + 1%K^+	1200	27

The microstructure investigations can explain the evolution of the porosity for each sample. The SEM images of fractures of 1000 °C, 1100 °C, and 1200 °C sintered samples are presented in Figure 2. These show the shape and the dimensions of crystallites and the absence of the secondaryphase. For the samples containing $Mg_{0.5}Zn_{0.5}Fe_2O_4$ + 1%Li^+, the increase of crystallites dimension is inhibited by the lithium cations segregation.

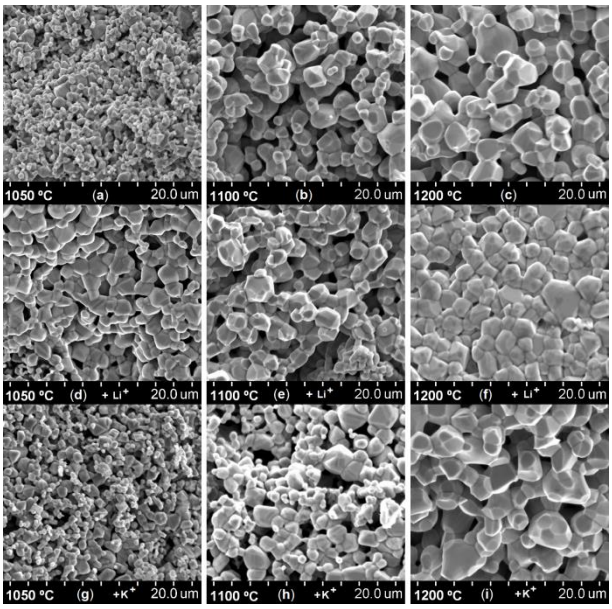

Figure 2. SEM images of the magnesium-zinc ferrites before and after thermal treatment (t = 4h) and cations addition (**a**) T = 1000 °C; (**b**) T = 1100 °C; (**c**) T = 1200 °C; (**d**) 1% Li^+, T=1000 °C; (**e**) 1% Li^+, T = 1100 °C; (**f**) 1% Li^+, T = 1200 °C; (**g**) 1% K^+, T = 1000 °C; (**h**) 1% K^+, T = 1100 °C; (**i**) 1% K^+, T = 1200 °C.

Moreover, we observed the influence of K^+, which alloweda fine-grained structure of the sample, and that the granulation can be increased by increasing the annealing temperature.

The 3D topographic profile of the surface of the Mg-Zn ferrite sample was made using a non-contact optical profilometer model ZygoZeGage at room temperature and pressure. Figure 3 shows the representative parameters of the calculated sample area: R_a—represents the arithmetic area; S_a—represents the mathematical area of the pixels; S_q—represents the square area of the pixels, and S_z—represents the topographic difference between the highest and lowest point. Analyzing the surface topography of the ferrite sample shown in Figure 3, we noticed that the surface is uniform and, in some places, has present agglomerations of crystallites, which is in agreement with the SEM micrographs shown in Figure 2.

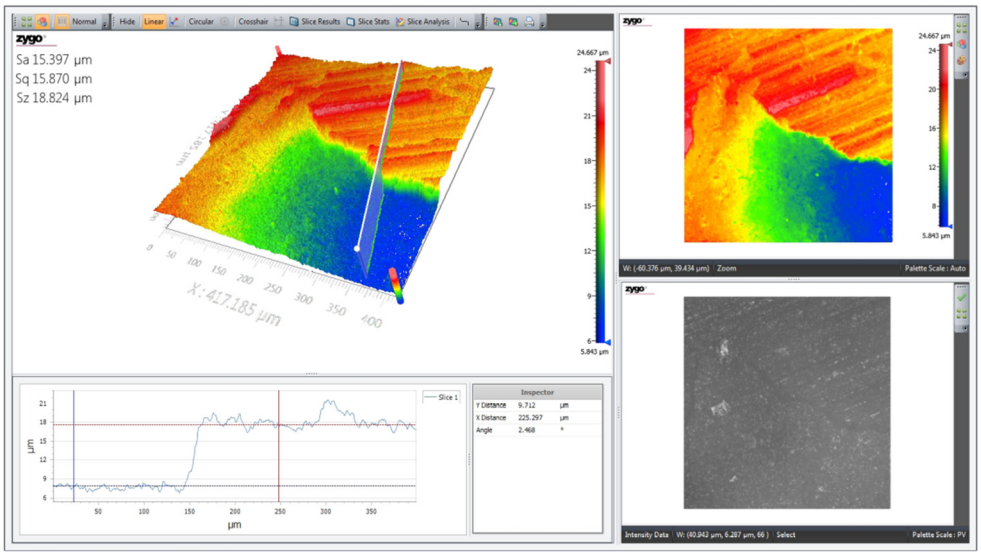

Figure 3. The 3D topographic surface profile of $Mg_{0.5}Zn_{0.5}Fe_2O_4$ ferrite sintered at 1100 °C.

3.2. Magnetic Properties

It is a well-known fact that the magnetization of ferrites depends on factors such as the addition or substitution of different cations in the ferrite composition, iron cations distributions between the A and B sites of the spinel structure, inhomogeneities, or crystallites size [17,36].

We found that the magnetic properties are influenced by the type of the additions and the annealing temperature. The specific saturation magnetization M_s was measured with a vibrating sample magnetometer in a magnetic field range −900–900 kA/m using spheres prepared from the pellet samples.

The investigation of magnetic properties confirmed that Mg-Zn ferrites are soft magnetic materials with high magnetic permeability and near to zero values for coercivity H_c (Figure 4).That is in concordance with results reported in the literature [21,32,37–40].

For the reference composition $Mg_{0.5}Zn_{0.5}Fe_2O_4$, sintered at 1000 °C for 4 h, the saturation value is high (45 emu/g), and remanence values are low (1.9 emu/g), as shown in Figure 4. For the same composition, changing the annealing temperature to 1100 °C results in the remanence having a significant increase to 2.7 emu/g (almost 45%), and the saturation rises to 56.8 emu/g. At a higher annealing temperature (1200 °C) used in the sample preparation, the remanent magnetization decreases to 1.5 emu/g, accompanied by a lowering of the saturation. Therefore, for the reference $Mg_{0.5}Zn_{0.5}Fe_2O_4$ ferrite, the optimal annealing temperature for increasing both M_r and M_s is 1100 °C.

In the case of ferrites having Li^+ cations included in the composition and sintered at 1000 °C, the measured value for saturation magnetization was 62.9 emu/g, and remanence magnetization was 2.8 emu/g. Relative to the reference sample, M_s and M_r were increased in the presence of Li^+ cations (Figure 4).

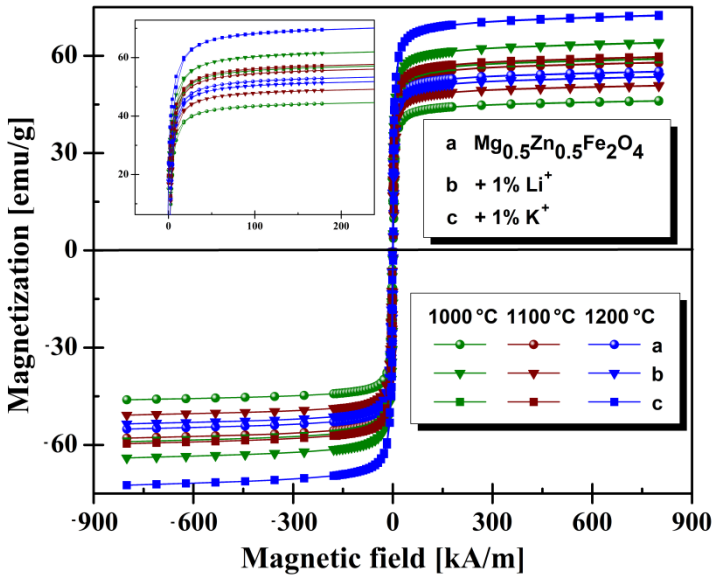

Figure 4. Magnetic hysteresis loops M (H) at room temperature obtained for investigated magnesium-zinc ferrites.

The change in annealing temperature from 1000 °C to 1100 °C led to a decrease inmagnetic properties. The explanation for this decrease is linked to the action of Li^+ cations upon grain size, in the sense of their diminishing. The annealing temperature of 1200 °C slightly increasedthe magnetic parameters at values lower than those of 1000 °C but comparable with values of the reference sample at the same temperature.

Magnetic properties of $Mg_{0.5}Zn_{0.5}Fe_2O_4$ with K^+ cations (Figure 4), sintered at 1000 °C, are comparable to ferrites with Li^+ cations, and therefore higher than the reference sample. Comparing the SEM images of sample structure, the change in granulation is one possible explanation. Grains of ferrites with K^+ cations, obtained at 1200 °C, are much more coarse and faceted compared to the reference sample (Figure 2c).

The relevant magnetic properties extracted from hysteresis measurement are summarized in Table 2. We found that the addition of metal cations to the composition of magnesium-zinc ferrite involved a significant increase of coercivity for all samples.

Table 2. Summary of the magnetic properties of Mg-Zn ferrites.

Sample	Annealing Temperature [°C]	Saturation M_s [emu/g]	Remanence M_R [emu/g]	Coercivity H_C [kA/m]
$Mg_{0.5}Zn_{0.5}Fe_2O_4$	1000	45.0	1.9	1.1
$Mg_{0.5}Zn_{0.5}Fe_2O_4$	1100	56.8	2.7	1.3
$Mg_{0.5}Zn_{0.5}Fe_2O_4$	1200	55.0	1.5	1.2
$Mg_{0.5}Zn_{0.5}Fe_2O_4$ + 1%Li^+	1000	62.9	2.8	7.1
$Mg_{0.5}Zn_{0.5}Fe_2O_4$ + 1%Li^+	1100	49.7	1.3	5.7
$Mg_{0.5}Zn_{0.5}Fe_2O_4$ + 1%Li^+	1200	52.4	1.5	6.2
$Mg_{0.5}Zn_{0.5}Fe_2O_4$ + 1%K^+	1000	57.9	2.2	8.7
$Mg_{0.5}Zn_{0.5}Fe_2O_4$ + 1%K^+	1100	59.5	2.5	8.9
$Mg_{0.5}Zn_{0.5}Fe_2O_4$ + 1%K^+	1200	72.3	3.1	9.2

As can be seen in Table 2, the intermediate temperature values are comparable with reference, but a spectacular increase is observed at 1200 °C, where the value of M_s is 72.3 emu/g, and M_r is 3.1 emu/g. The variations of the magnetic parameters may be ascribed to compositional perturbations produced by the presence of atoms Li^+ or K^+ in the host spinel lattice. This results in a magnetic dilution of the octahedral sublattice. A significant increase of saturation is observed for ferrites sintered at 1000 °C, where the addition of Li^+ cations causes an increase of saturation by over 39%, and for ferrites sintered at 1200 °C, the addition of K^+ cations causes an increase of saturation by over 31%. Comparing our magnetic properties with the results reported by T. Tatarchuk [21],

it is found that the addition of Li^+ and K^+ cations to the Mg-Zn spinel ferrite implies the obtaining of superior magnetic properties. Thus, the increase of values in the case of saturation (M_s) and coercivity (H_c) is observed.

3.3. Dielectric Properties

For applications in the field of electronics, the dependence on the electrical permittivity of the frequency is very important. In the case of spinel ferrites, the number of Fe^{2+} ions placed in octahedral sites of lattices plays an important role in the conduction mechanism. The electronic conduction mechanism is based on electron exchanges between ions of the same species that are randomly distributed and have different valence states.

The measurements on the frequency dependence of electrical permittivity are presented in Figure 5. We found that the compositional and annealing temperature changes also influenced the electrical permittivity. High values at low frequency for the real part of permittivity confirm the semiconducting characteristic of this category of materials. These characteristics were also reported in the literature [41,42]. The remarkable case is, in our investigation, the Mg-Zn ferrites with K^+ cations. For 1100 °C annealed samples, the real permittivity value is nearly constant in the range of frequencies 1–100 Hz. Increasing the sintering temperature to 1200 °C, this constant interval is extended to 10^5 Hz (Figure 5).

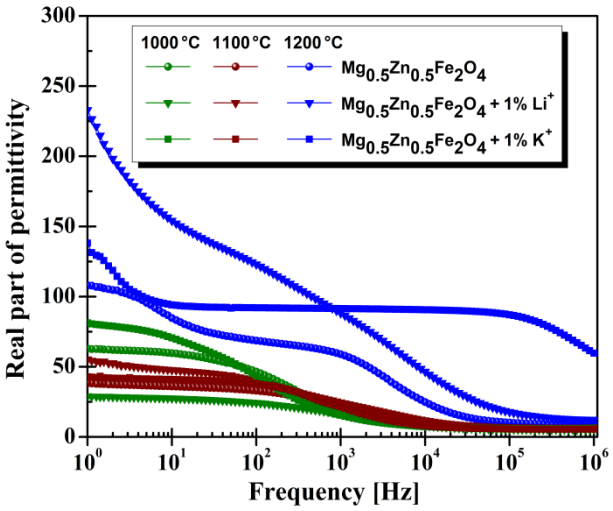

Figure 5. Dielectric characteristics of the Mg-Zn ferrites.

For all samples, the imaginary part of permittivity exponentially decreases in the range 1–10^6 Hz, with a quick tendencyat low frequencies, 1–10 Hz, and a slow one from 10^2 to 10^6 Hz (Figure 6). Similar results were reported in the literature by [43,44].

A Wayne Kerr Impedance Phase Analyzer was used to investigate the variation of the electric permittivity in the frequency range $10^7 \div 10^9$ Hz.

As can be seenin Figure 7, high frequency, unlike low frequency, samples treated at high temperatures showed high values of permittivity. As shown in Figure 7, in the range 10^7–10^9 Hz, the real part of permittivity (ε') remains constant for all analyzed samples, which means good stability to a higher frequency. Similar behavior of dielectric constant was also reported in the literature [19]. Comparing our dielectric properties with the results reported by M.A.Rahman [19] found that the addition of Li^+ and K^+ cations to Mg-Zn spinel ferrite obtained superior dielectric properties.Thus, a doubling of the values of the dielectric constant for the high-frequency domain was observed. Also, it was observed that added cations in the Mg-Zn ferrite increased the real part of permittivity; the highest values were observed for Li^+ added cations, irrespective of temperature treatment. The same rules can also be observed in the case of the imaginary part of permittivity (see Figure 8).

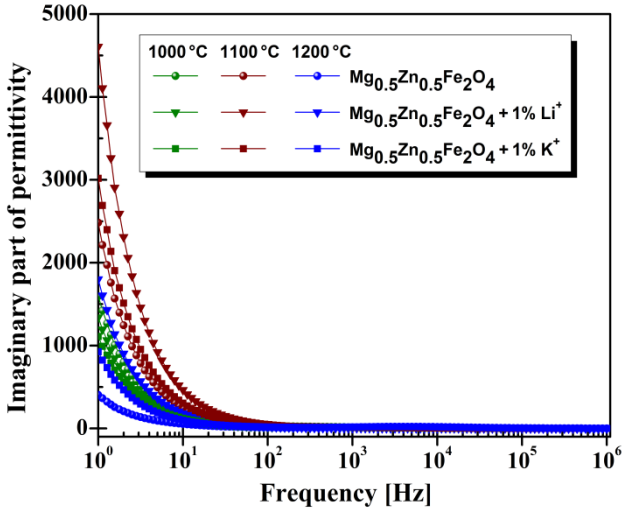

Figure 6. Imaginary part of permittivity vs. frequency for investigated magnesium-zinc ferrites.

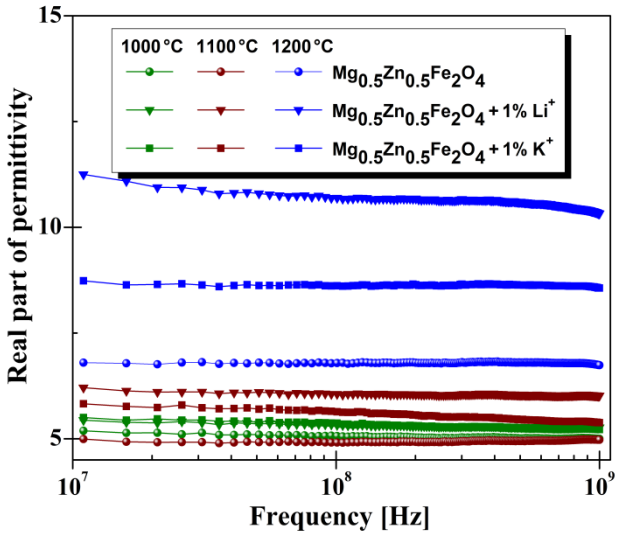

Figure 7. High-frequency characteristics of real part of permittivity for investigated Mg-Zn ferrite.

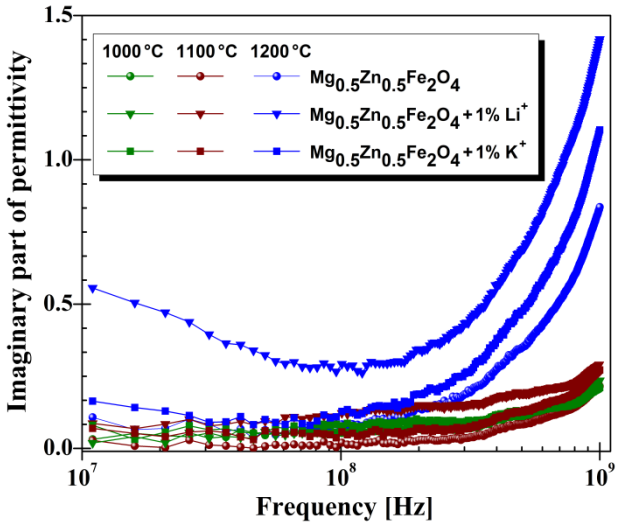

Figure 8. High-frequency characteristics of imaginary part of permittivity for investigated Mg-Zn ferrites.

The influence of temperature treatment on the dielectric losses can be observed for all samples at very high frequency, in that high-temperature treatment increases the value of imaginary part of permittivity (ε'') near to 10^9 Hz.

4. Conclusions

In this paper, we show that porous Mg-Zn ferrite can be obtained at medium temperatures using the addition of alkaline metal cations. The different behaviors of the samples are caused by the annealing temperature and different microstructures in close correlation with the action of the cations additions.

As a result of studies, we found that the physical parameters of Mg-Zn ferrite are more or less influenced by the presence of foreign cations introduced as additives to the structure of ferrite. The study of the Mg-Zn ferrite with spinel structure was determined by the necessity to obtain good porosity, superior magnetic or electrical properties by performing controlled additions of Li^+ and K^+ cations to the host composition of the ferrite.

The annealing temperature and type of added cations play an important role in the modification of the microstructure, magnetic, and dielectric properties.

We found that the porosity of all samples decreases with increased annealing temperature due to the increase of particle grain size. Significant increases in porosity are observed for samples sintered at 1200 °C, where the addition of Li+ cations involves an increase of porosity by 20%, and the addition of K+ cations involves an increase of porosity by 35% compared with the reference sample.

Significant increases of saturation are observed for ferrites sintered at 1000 °C, where the addition of Li^+ cations causes an increase of saturation by over 39%, and for ferrites sintered at 1200 °C, the addition of K^+ cations causes an increase of saturation by over 31%.

Another important result is the constant value for dielectric permittivity in the frequency range of 10–10^5 Hz for $Mg_{0.5}Zn_{0.5}Fe_2O_4$ ferrites with the addition of K^+, annealed at 1200 °C.

We demonstrated that by selecting an appropriate cationic addition or by choosing an optimal sintering temperature, it might be possible to improve the magnetic and electrical properties of Mg-Zn ferrite.

Author Contributions: Conceptualization, I.P. and F.T.; methodology, I.P. and F.T.; validation, I.P. and F.T.; formal analysis, I.P. and F.T.; investigation, I.P. and F.T.; writing—original draft preparation, I.P. and F.T.; writing—review and editing, I.P. and F.T.; visualization, I.P. and F.T.; All authors have read and agreed to the published version of the manuscript.

Funding: This research was funded by Ministry of Research, Innovation and Digitization, grant number CNFIS-FDI-2021-0501.

Institutional Review Board Statement: Not applicable.

Informed Consent Statement: Not applicable.

Data Availability Statement: Exclude this statement.

Acknowledgments: This work was supported by a grant of the Ministry of Research, Innovation and Digitization, CNCS/CCCDI-UEFISCDI, project number: CNFIS-FDI-2021-0501.

Conflicts of Interest: The authors declare no conflict of interest.

References

1. Kuru, M.; Kuru, T.S.; Karaca, E.; Bagcı, S. Dielectric, magnetic and humidity properties of Mg-Zn-Cr ferrites. *J. Alloy. Compd.* **2020**, *836*, 15531. [CrossRef]
2. Fantozzi, E.; Rama, E.; Calvio, C.; Albini, B.; Galinetto, P.; Bini, M. Silver doped magnesium ferrite nanoparticles: Physico-chemical characterization and antibacterial activity. *Materials* **2021**, *14*, 2859. [CrossRef]
3. Tudorache, F. Investigations on microstructure, electrical and magnetic properties of copper spinel ferrite with WO_3 addition for applications in the humidity sensors. *Superlattices Microstruct* **2018**, *116*, 131–140.

4. Omelyanchik, A.; Levada, K.; Pshenichnikov, S.; Abdolrahim, M.; Baricic, M.; Kapitunova, A.; Galieva, A.; Sukhikh, S.; Astakhova, L.; Antipov, S.; et al. Green synthesis of Co-Zn spinel ferrite nanoparticles: Magnetic and intrinsic antimicrobial properties. *Materials* **2020**, *13*, 5014. [CrossRef]
5. Bugad, R.A.; Bansode, P.A.; Karche, B.R. Influences of La^{3+} ion substitution on dielectric, susceptibility and permeability properties of Mg–Zn ferrite nanoparticles. *J. Mater. Sci. Mater. Electron.* **2020**, *27*, 1–14. [CrossRef]
6. Tudorache, F.; Petrila, I. Effects of partial replacement of Iron with Tungsten on microstructure, electrical, magnetic and humidity properties of Copper-Zinc ferrite material. *J. Electron. Mater.* **2014**, *43*, 3522–3526. [CrossRef]
7. Sharma, R.; Thakur, P.; Sharma, P.; Sharma, V. Mn^{2+} doped Mg-Zn ferrite nanoparticles for microwave device applications. *IEEE Electron. Device Lett.* **2018**, *39*, 901–904. [CrossRef]
8. Klekotka, U.; Satuła, D.; Spassov, S.; Szostko, B.K. Influence of atomic doping on thermal stability of ferrite nanoparticles—structural and magnetic studies. *Materials* **2021**, *14*, 100. [CrossRef] [PubMed]
9. Rezlescu, N.; Tudorache, F.; Rezlescu, E.; Popa, P.D. The effect of the additives and sintering temperature on the structure and humidity sensitivity of a spinel ferrite. *J. Optoelectron. Adv. Mater.* **2008**, *10*, 2386–2389.
10. Cherpin, C.; Lister, D.; Dacquait, F.; Liu, L. Study of the solid-state synthesis of nickel ferrite ($NiFe_2O_4$) by X-ray diffraction (XRD), scanning electron microscopy (SEM) and Raman spectroscopy. *Materials* **2021**, *14*, 2557. [CrossRef]
11. Das, B.C.; Alam, F.; Akther, A.K.M.H. The crystallographic, magnetic, and electrical properties of Gd^{3+}-substituted Ni-Cu-Zn mixed ferrites. *J. Phys. Chem. Solids* **2020**, *142*, 109433. [CrossRef]
12. Kuru, T.S. Synthesis and investigation of structural, dielectric, impedance, conductivity and humidity sensing properties of Cr^{3+}-substituted Mg-Zn ferrite nanoparticle. *Appl. Phys. A Mater. Sci. Process.* **2020**, *126*, 419. [CrossRef]
13. Li, J.; Yang, Y.; Wang, G.; Guo, L.; Rao, Y.H.; Gan, G.W.; Zhang, H.W. Enhanced structure and microwave magnetic properties of MgZn ferrite by Cd^{2+} ion substitution for LTCC applications. *Ceram. Int.* **2020**, *46*, 6600–6604. [CrossRef]
14. Ali, M.A.; Khan, M.N.I.; Hossain, M.M.; Chowdhury, F.U.Z.; Hossain, M.N.; Rashid, R.; Hakim, M.A.; Hoque, S.M.; Uddin, M.M. Mechanical behavior, enhanced dc resistivity, energy band gap and high temperature magnetic properties of Y-substituted Mg–Zn ferrites. *Mater.Res.Express.* **2020**, *7*, 036101. [CrossRef]
15. Rezlescu, N.; Rezlescu, E.; Tudorache, F.; Popa, P.D. MgCu nanocrystalline ceramic with La^{3+} and Y^{3+} ionic substitution used as humidity sensor. *J. Optoelectron. Adv. Mater.* **2004**, *6*, 695–698.
16. Manikandan, V.; Singh, M.; Yadav, B.C.; Mane, R.S.; Vigneselvan, S.; Mirzaei, A.; Chandrasekaran, J. Room temperature LPG sensing properties of tin substituted copper ferrite (Sn-$CuFe_2O_4$) thin film. *Mater. Chem. Phys.* **2020**, *240*, 122265. [CrossRef]
17. Khot, S.S.; Shinde, N.S.; Ladgaonkar, B.P.; Kale, B.B.; Watawe, S.C. Magnetic and structural properties of Magnesium Zinc ferrites synthesized at different temperature. *Adv. Appl. Sci. Res.* **2011**, *2*, 460–471.
18. Ali, M.A.; Khan, M.N.I.; Chowdhury, F.U.Z.; Hossain, M.M.; Rahaman, M.Z.; Hoque, S.M.; Matin, M.A.; Uddin, M.M. Study of physical properties towards optimizing sintering temperature of Y-substituted Mg-Zn ferrites. *Results Phys.* **2019**, *14*, 102517. [CrossRef]
19. Rahman, M.A.; Islam, M.T.; Singh, M.S.J.; Chowdhury, M.E.H.; Samsuzzaman, M. Quad-band flexible magnesium zinc ferrite ($MgZnFe_2O_4$)-based double negative metamaterial for microwave applications. *Chin. J. Phys.* **2021**, *71*, 351–364. [CrossRef]
20. Sajjad, M.; Ali, K.; Javed, Y.; Sattar, A.; Akbar, L.; Nawaz, A.; Rashid, M.Z.; Rasool, K.; Alzaid, M. Detailed analysis of structural and optical properties of spinel cobalt doped magnesium zinc ferrites under different substitutions. *J. Mater. Sci. Mater. Electron.* **2020**, *31*, 21779–21791. [CrossRef]
21. Tatarchuk, T.; Myslin, M.; Lapchuk, I.; Shyichuk, A.; Murthy, A.P.; Gargula, R.; Kurzydło, P.; Bogacz, B.F.; Pędziwiatr, A.T. Magnesium-zinc ferrites as magnetic adsorbents for Cr(VI) and Ni(II) ions removal: Cation distribution and antistructure modeling. *Chemosphere* **2021**, *270*, 129414. [CrossRef] [PubMed]
22. Petrova, E.; Kotsikau, D.; Pankov, V.; Fahmi, A. Influence of synthesis methods on structural and magnetic characteristics of Mg–Zn-ferrite nanopowders. *J. Magn. Magn. Mater.* **2019**, *473*, 85–91. [CrossRef]
23. Yadav, A.; Varshney, D. Structural and dielectric properties of copper-substituted Mg-Zn spinel ferrites. *J. Supercond. Nov. Magn.* **2017**, *30*, 1297–1302. [CrossRef]
24. Ghodake, U.R.; Chaudhari, N.D.; Kambale, R.C.; Patil, J.Y.; Suryavanshi, S.S. Effect of Mn^{2+} substitution on structural, magnetic, electric and dielectric properties of Mg-Zn ferrites. *J. Magn. Magn. Mater.* **2016**, *407*, 60–68. [CrossRef]
25. Reyes-Rodriguez, P.Y.; Cortes-Hernandez, D.A.; Escobedo-Bocardo, J.C.; Almanza-Robles, J.M.; Sanchez-Fuentes, H.J.; Jasso-Teran, A.; De Leon-Prado, L.E.; Mendez-Nonell, J.; Hurtado-Lopez, G.F. Structural and magnetic properties of Mg-Zn ferrites ($Mg_{1-x}Zn_xFe_2O_4$) prepared by sol-gel method. *J. Magn. Magn. Mater.* **2017**, *427*, 268–271. [CrossRef]
26. Henaish, A.M.A. Physical and spectral studies of Mg-Zn ferrite prepared using different methods. *Arab. J. Nucl. Sci. Appl.* **2020**, *53*, 9–18.
27. Tatarchuk, T.; Myslin, M.; Mironyuk, I.; Bououdina, M.; Pedziwiatr, A.T.; Gargula, R.; Bogacz, B.F.; Kurzydlo, P. Synthesis, morphology, crystallite size and adsorption properties of nanostructured Mg-Zn ferrites with enhanced porous structure. *J. Alloys Compd.* **2020**, *819*, 152945. [CrossRef]
28. Sharma, R.; Thakur, P.; Kumar, M.; Sharma, P.; Sharma, V. Nanomaterials for high frequency device and photocatalytic applications: Mg-Zn-Ni ferrites. *J. Alloys Compd.* **2018**, *746*, 532–539. [CrossRef]
29. Mezher, S.J.; Kadhim, K.J.; Abdulmunem, O.M.; Mejbel, M.K. Microwave properties of Mg-Zn ferrite deposited by the thermal evaporation technique. *Vacuum* **2020**, *173*, 109114. [CrossRef]

30. Kumar, P.; Khadtare, S.; Park, J.; Yadav, B.C. Fabrication of leaf shaped SnO_2 nanoparticles via sol-gel route and its application for the optoelectronic humidity sensor. *Mater. Lett.* **2020**, *278*, 128451. [CrossRef]
31. Petrila, I.; Tudorache, F. Humidity sensor applicative material based on copper-zinc-tungsten spinel ferrite. *Mater. Lett.* **2013**, *108*, 129–133. [CrossRef]
32. Ali, M.A.; Khan, M.N.I.; Chowdhury, F.U.Z.; Hossain, M.M.; Hossain, A.K.M.A.; Rashid, R.; Nahar, A.; Hoque, S.M.; Matin, M.A.; Uddin, M.M. Yttrium-substituted Mg-Zn ferrites: Correlation of physical properties with Yttrium content. *J. Mater. Sci. Mater. Electron.* **2019**, *30*, 13258–13270. [CrossRef]
33. Sharma, R.; Thakur, P.; Kumar, M.; Barman, P.B.; Sharma, P.; Sharma, V. Enhancement in A-B super-exchange interaction with Mn^{2+} substitution in Mg-Zn ferrites as a heating source in hyperthermia applications. *Ceram. Int.* **2017**, *43*, 13661–13669. [CrossRef]
34. Debnath, S.; Deb, K.; Saha, B.; Das, R. X-ray diffraction analysis for the determination of elastic properties of zinc-doped manganese spinel ferrite nanocrystals ($Mn_{0.75}Zn_{0.25}Fe_2O_4$), along with the determination of ionic radii, bond lengths, and hopping lengths. *J. Phys. Chem. Solids* **2019**, *134*, 105–114. [CrossRef]
35. Hirosawa, F.; Iwasaki, T.; Watano, S. Synthesis and magnetic induction heating properties of Gd-substituted Mg-Zn ferrite nanoparticles. *Appl.Nanosci.* **2017**, *7*, 209–214. [CrossRef]
36. Mazen, S.A.; Mansour, S.F.; Zaki, H.M. Some physical and magnetic properties of Mg-Zn ferrite. *Cryst. Res. Technol.* **2003**, *38*, 471–478. [CrossRef]
37. Da Dalt, S.; Takimi, A.S.; Volkmer, T.M.; Sousa, V.C.; Bergmann, C.P. Magnetic and Mössbauerbehavior of the nanostructured $MgFe_2O_4$ spinel obtained at low temperature. *Powder Technol.* **2011**, *210*, 103–108. [CrossRef]
38. Nakamura, T. Snoek's limit in high-frequency permeability of polycrystalline Ni–Zn, Mg–Zn, and Ni–Zn–Cu spinel ferrites. *J. Appl. Phys.* **2000**, *88*, 348–353. [CrossRef]
39. Mukhtar, M.W.; Irfan, M.; Ahmad, I.; Ali, I.; Akhtar, M.N.; Khan, M.A.; Abbas, G.; Rana, M.U.; Ali, A.; Ahmad, M. Synthesis and properties of Pr-substituted MgZn ferrites for core materials and high frequency applications. *J. Magn. Magn. Mater.* **2015**, *381*, 173–178. [CrossRef]
40. Bharti, D.C.; Mukherjee, K.; Majumder, S.B. Wet chemical synthesis and gas sensing properties of magnesium zinc ferrite nano-particles. *Mater. Chem. Phys.* **2010**, *120*, 509–517. [CrossRef]
41. Sivakumar, N.; Narayanasamy, A.; Greneche, J.-M.; Murugaraj, R.; Lee, Y.S. Electrical and magnetic behaviour of nanostructured $MgFe_2O_4$spinel ferrite. *J. Alloys Compd.* **2010**, *504*, 395–402. [CrossRef]
42. Murase, T.; Igarashi, K.; Sawai, J.; Nomura, T. Relaxation phenomena of MgZn ferrites. *J. Phys. IV* **1997**, *C1*, 99–100. [CrossRef]
43. Ghodake, U.R.; Kambale, R.C.; Suryavanshi, S.S. Effect of Mn^{2+} substitution on structural, electrical transport and dielectric properties of Mg-Zn ferrites. *Ceram. Int.* **2017**, *43*, 1129–1134. [CrossRef]
44. Wu, G.; Yu, Z.; Sun, K.; Guo, R.; Jiang, X.; Wu, C.; Lan, Z. Effect of $CaCu_3Ti_4O_{12}$dopant on the magnetic and dielectric properties of high-frequency MnZn power ferrites. *J. Magn. Magn. Mater.* **2020**, *513*, 167095. [CrossRef]